Phase transitions in CdTe to 28 GPa

R. J. Nelmes, M. I. McMahon, N. G. Wright, and D. R. Allan
Department of Physics and Astronomy, The University of Edinburgh, Mayfield Road, Edinburgh EH9 3JZ, United Kingdom
(Received 1 August 1994)

Angle-dispersive powder-diffraction techniques utilizing an image-plate area detector and synchrotron radiation have been used to study the phase transitions in CdTe above 8 GPa. The well-known phase transition at 10 GPa is not to the β-tin structure as has previously been reported, but to an orthorhombic structure with space group *Cmcm*. This is the same structure as recently reported for ZnTe-III, and is characterized by a fivefold coordination of close nearest neighbors. The *Cmcm* phase is stable to at least 28 GPa, and the pressure dependence of the structure has been determined over this range. The continuous nature of the NaCl→*Cmcm* transition, coupled with the limited resolution and lower sensitivity of previous studies, accounts for the earlier reports of a β-tin phase, and of a transition at 12 GPa from the supposed β-tin phase to an orthorhombic phase with space group *Pmm*2.

INTRODUCTION

The generally accepted transition sequence yielded by experimental and theoretical studies of II-VI semiconductors is zincblende (or wurtzite)→NaCl→β-tin with increasing pressure.[1] And the more ionic III-V systems, like InAs, have been found to behave the same way.[2] The main exceptions are that the NaCl phase is preceded by a cinnabar phase in the HgX compounds,[1] and that the high-pressure phases of ZnTe appear to be more complex.[3–5] In the case of CdTe, the basic sequence has been well documented for some 30 years, with the zincblende (CdTe-I)→NaCl (CdTe-II) transition occurring at 3.5 GPa,[6–8] and the NaCl→β-tin (CdTe-III) transition at ~10 GPa.[7,8] A further transition, to an orthorhombic structure with space group *Pmm*2 (CdTe-IV), has been reported at ~12 GPa.[9]

There is now growing evidence that this picture is incomplete, and in some respects incorrect. Using angle-dispersive diffraction techniques and synchrotron radiation, we have shown[10,11] that in fact CdTe has *two* closely spaced transitions near 3.5 GPa: first zincblende to cinnabar and then cinnabar to NaCl. A cinnabar phase has also been found in ZnTe at high pressure (ZnTe-II).[3–5,12] And our preliminary studies of HgTe-IV, CdTe-IV, and ZnTe-III at ~18 GPa have shown[13] that the diffraction patterns from all three materials are incompatible with their previously reported structures (β-tin, *Pmm*2, and monoclinic, respectively). The patterns did, however, possess many similarities, and could all be indexed on a *C*-face-centered-orthorhombic unit cell. Subsequent detailed diffraction studies of ZnTe-III have shown[12] the structure to be a strong distortion of the NaCl structure, with space group *Cmcm*.

In order to investigate the structural phase transitions in CdTe above 5 GPa, and to determine the structural relationship, if any, of CdTe-III and CdTe-IV with ZnTe-III, we have performed detailed angle-dispersive diffraction measurements on CdTe to 28 GPa. We find that at 10 GPa the NaCl phase of CdTe transforms continuously into a *Cmcm* structure that is stable to at least 28 GPa. Neither the β-tin nor *Pmm*2 phases are found to exist. The observation of a *Cmcm* structure in ZnTe and CdTe marks the emergence of new structural systematics in the II-VI semiconductors.

EXPERIMENTAL DETAILS

Diffraction data were collected on station 9.1 at the Synchrotron Radiation Source, Daresbury, using angle-dispersive diffraction techniques and an image-plate area detector. In order to enhance the difference in scattering power between the Cd ($Z=48$) and Te ($Z=52$) atoms, we used an incident wavelength of 0.4652(1) Å, 59 eV from the measured position of the Cd K-absorption edge. The incident monochromatic beam was collimated by a platinum pinhole to a diameter of 75 μm. Great care was taken to minimize contaminant and background scattering. The two-dimensional Debye-Scherrer patterns were collected on Kodak image plates and read on a Molecular Dynamics 400A PhosphorImager, using a pixel size of 88×86 μm^2, and then integrated to give conventional one-dimensional diffraction profiles. Details of our experimental setup, alignment procedure, and pattern integration software have been reported previously.[14,15]

The progressive discovery of the nature of the high-pressure behavior led to a large number of data points being obtained through the range up to 18 GPa, with data collected from five different CdTe samples. All the samples were prepared from the same starting material of >99.99% purity provided by the Aldrich Chemical Company. For studies to 14 GPa, we employed Merrill-Bassett diamond-anvil pressure cells (DAC's) with diamond culet diameters of 600 μm. These DAC's permit the pressure to be increased in very small increments of 0.1–0.2 GPa, which was essential in the study of the small and gradual peak splittings observed immediately above 10 GPa. For studies to 28 GPa, we employed a Diacell-DXR4 DAC (Ref. 16) with diamond culet diameters of 300 μm. Both types of DAC have full conical apertures of $\geq 40°$. In all cases the samples were loaded into 150–200 μm holes in tungsten gaskets with a 4:1

0163-1829/95/51(22)/15723(9)/$06.00

mixture of methanol:ethanol as a pressure-transmitting fluid. The pressure was measured before and after each exposure using the ruby fluorescence technique.[17]

The structural results were obtained in almost all cases by full Rietveld refinement[18] of the integrated profiles using the program MPROF.[19] However, no stable solution was possible using Rietveld techniques for the high-pressure phase just above 10 GPa—where the extra lines are very weak—and lattice parameters were obtained instead by least-squares analysis of measured d spacings. Since full refinements could not be carried out, values of the atomic coordinates were not obtained at these pressures (10.3 and 10.7 GPa).

RESULTS AND DISCUSSION

On pressure increase, the NaCl structure of CdTe was observed from 3.8 to 10 GPa. Very weak extra reflections began to appear in the diffraction profiles at 10.1 GPa, and grew in intensity as the pressure was increased. Figure 1 shows the integrated profile obtained at 11.7 GPa, and A and B mark the strongest of the new reflections. As shown in the inset, five further new reflections are discernible, but only A and B have been observed in the three previous studies of CdTe above 10 GPa.[7–9] In each case the authors indexed them as the (101) and (211) reflections, respectively, from a β-tin structure. The (200) and (220) reflections from the β-tin phase—which have intensities comparable with (101) and (211), respectively, and should thus also be clearly visible—were assumed to be overlapped by the (200) and (220) reflections of the NaCl phase in a mixed-phase NaCl/β-tin sample. If the 11.7 GPa profile is analyzed this way—using the measured d spacings of the NaCl (111), (200), (220), and (222), and the β-tin (101) and (211) reflections—the refined lattice parameters are $a=5.761(2)$ Å, and $a=5.761(2)$ Å and $c=2.911(2)$ Å for the NaCl and β-tin phases, respectively. However, a NaCl/β-tin mixed-phase profile accounts for only three of the seven newly observed reflections; the four that are not accounted for are indicated by asterisks in inset (i) of Fig. 1.

Close examination of the profile collected at 11.7 GPa reveals that the peak at $2\theta\approx 9.3°$ [the (200) reflection in the NaCl phase] is clearly asymmetric, as illustrated in inset (ii) in Fig. 1. Further increases in pressure resulted first in increased asymmetry and then in a splitting of this reflection, with a new peak shifting to smaller 2θ angles (longer d spacing). This is illustrated in Fig. 2 which shows a sequence of profiles obtained at pressures between 11.2 and 13.6 GPa. The peak at $2\theta\approx 13°$ can also be seen to split over this pressure range. The splitting of the reflection at $2\theta\approx 9.3°$, and the shift of the new reflection to longer d spacing, was observed previously by Hu,[9] who interpreted it as evidence of a transition from the β-tin phase to the orthorhombic $Pmm2$ phase at 12.18 GPa. However, analysis of profiles collected between 10 and 12 GPa, reveals that the asymmetry is evident at pressures as low as 10.9 GPa, indicating that the asymmetry accompanies the development of the non-NaCl reflections indicated in Fig. 1. The present data strongly suggest, therefore, that the phases previously reported as β-tin and $Pmm2$ are, in fact, one and the same, and that this phase does not have the β-tin structure.

The sample pressure was increased further to 18.6 GPa, and the profile shown in Fig. 3 was collected. In this pressure range the CdTe pattern is very similar to that found in ZnTe-III and HgTe-IV, as previously noted.[13] From the profile in Fig. 3, it was possible to determine the d spacings of 12 lines unambiguously. Autoin-

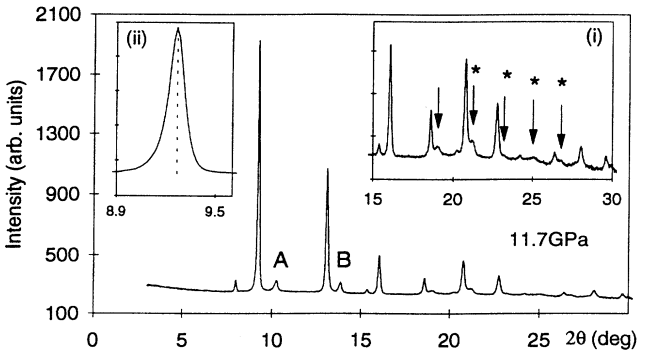

FIG. 1. Integrated profile of CdTe at 11.7 GPa. A and B mark the strongest of the non-NaCl reflections, while five weaker non-NaCl reflections are indicated by arrows in inset (i). Four of these latter reflections—indicated by asterisks—cannot be accounted for by a NaCl/β-tin mixed-phase profile. Inset (ii) shows an enlargement of the asymmetric peak in the main profile at $2\theta\sim 9.3°$.

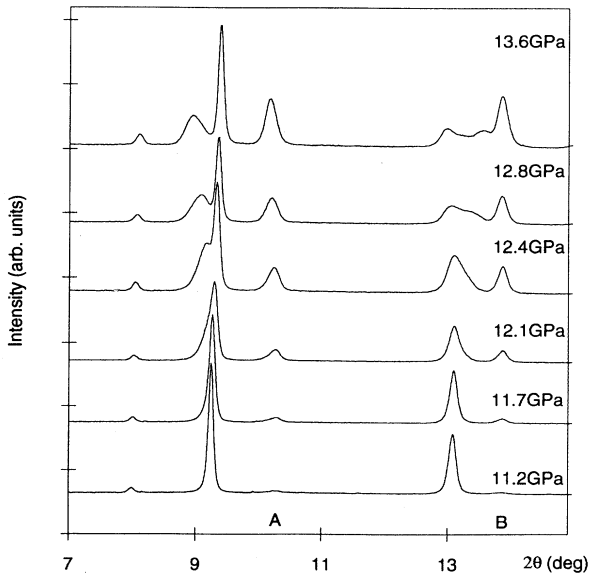

FIG. 2. The sequence of integrated profiles obtained from CdTe at pressures between 11.2 and 13.6 GPa. A and B mark the same two non-NaCl reflections as in Fig. 1.

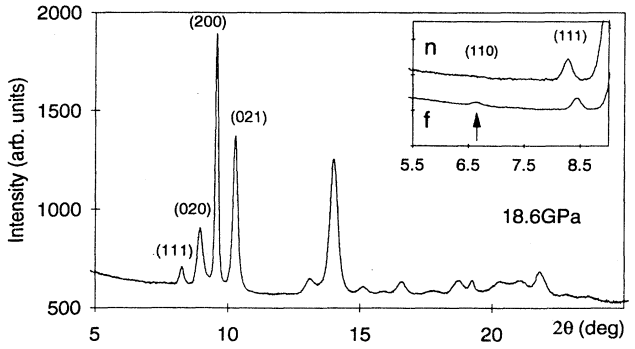

FIG. 3. Integrated profile of CdTe at 18.6 GPa. The inset shows an enlargement of the region of the profile close to the position of the (110) reflection recorded at 26.175 keV, far (f) from the Cd K edge, and at 26.656 keV, near (n) the Cd K edge (at 26.715 keV). The two profiles in the inset are on a common intensity scale.

dexing of these d spacings using the program DICVOL (Ref. 20) gave an excellent fit to the observed data with an orthorhombic unit cell having $a=5.58$ Å, $b=5.97$ Å, and $c=5.28$ Å. Indexing of the whole profile revealed that reflections with $h+k=$odd in all (hkl) and $l=$odd in ($h0l$) are systematically absent. The symmetry of the lattice is thus C-face centered, with a four-atom basis required to give a physically reasonable density.

As in the case of ZnTe-III,[12] solving the structure of CdTe is greatly facilitated by establishing the nature of the atomic ordering. The inset to Fig. 3 shows, on a common intensity scale, the region of the diffraction pattern close to the position of the (110) reflection recorded at incident wavelengths near to (n) and far from (f) the Cd K edge. Near the edge, the (110) reflection is almost absent, but it becomes clearly visible (although still very weak) away from the edge. There is also a change in the intensity of the (111) reflection which, by contrast, becomes weaker away from the edge. These clear intensity changes show the structure to be site ordered. The systematic absence conditions restrict the possible spacegroups to $Cmcm$, $C2cm$, and $Cmc2_1$ for atoms on general positions, but these three groups all have 8- and 16-fold general positions and the site ordering further restricts possible structures to ones with fourfold special positions. Only the 4(c) sites of $Cmcm$, the 4(b) sites of $C2cm$ and the 4(a) sites of $Cmc2_1$ are consistent with the observed absences. [The absences are also consistent with the 4(b) special position of $C222_1$, but this is not distinguishable from 4(c) of $Cmcm$ and therefore will not be considered further.]

The strong similarities with ZnTe-III suggest that initial structural refinements can be based on the ZnTe-III structure—that is, spacegroup $Cmcm$ with Cd at $\sim(0,0.7,0.25)$ and Te at $\sim(0,0.2,0.25)$. Trial refinements confirmed this as a plausible structure, but the (002) reflection is not observed in the profile although it has a calculated intensity similar to that of the nearby (021) reflection (see Fig. 3). This disagreement in intensities also results in a general misfit to the positions of other weaker peaks, because the refinement adjusts the lattice parameters so as to overlap the (002) and (021) reflections and thus minimize the overall disagreement between observed and calculated profiles. In our earlier study of ZnTe-III we found[12] that the intensity of the (002) reflection could be strongly affected by preferred orientation (PO) effects, although in the case of ZnTe the (002) was still clearly visible in the integrated profiles. Analysis of the 2-d images of CdTe obtained above 13 GPa revealed that the PO was *much* stronger than in ZnTe. Furthermore, strong intensity variations around the Debye-Scherrer rings revealed that the PO distribution was not coaxial with the pressure-cell axis.

In order to check whether the apparent absence of the (002) reflection was indeed due to the strong PO effects, profiles were collected with the axis of the pressure cell at various inclinations to the incident x-ray beam. Detection of (002) was facilitated by making these measurements at a pressure of 14 GPa, where the best estimates of the lattice parameters showed (002) to be well separated from both the (200) and the (021) reflections. Figure 4 shows profiles obtained from the same sample at inclination angles of 0° and 30°. It can be seen that not only does the (002) reflection become clearly visible when the DAC is inclined at 30°, but also the intensities of the (020), (021), and—less evidently from this figure—(200) reflections are significantly reduced. It is also evident that the (200) reflection is considerably sharper than the other reflections, and the same is true for (400). Such effects can arise as a consequence of the shape of the sam-

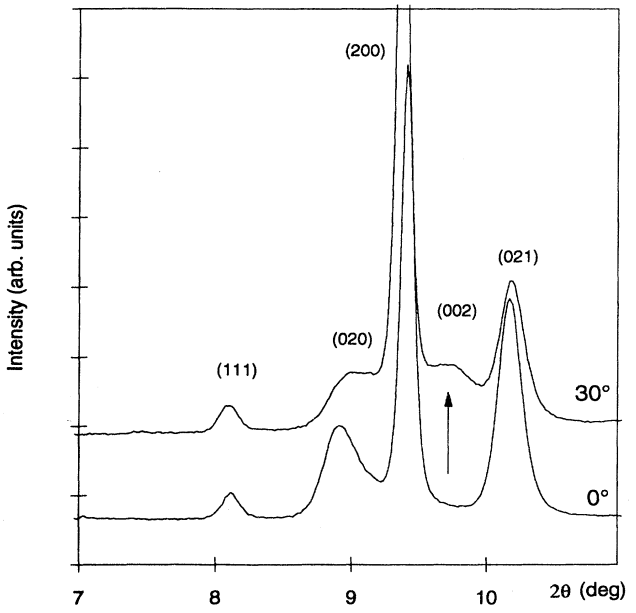

FIG. 4. Integrated profiles from the same CdTe sample at 14.0 GPa, obtained at sample-inclination angles of 0° and 30°. The arrow indicates the calculated position of the (002) reflection.

ple crystallites, with the sharp ($h00$) reflections suggestive of needlelike crystallites with their long axis parallel to [100].

Despite many attempts, it has not proved possible to obtain a sample in which the (002) reflection is visible in a noninclined DAC. This suggests that the strong PO effects arise as a consequence of the phase transition from the NaCl phase rather than sample preparation or the rate of pressure increase. Attempts to determine a preferred orientation correction that will reduce the calculated intensity of the (002) reflection to zero have also proved unsuccessful. This is not surprising: such extreme effects are outside the range over which the standard one-parameter March-Dollase[21] model used in the structure refinements with MPROF (Ref. 19) can give an accurate correction. However, trial refinements at several pressures show that there is little or no effect on the refined atomic coordinates if the (002) reflection is simply omitted from the refinement, and so this was done in all cases.[22] Removing the (002) also has the benefit of improving the overall fit to the observed profile by eliminating the distortion of the unit cell that results from trying to overlap the (002) and (021) reflections, as discussed above.

The variables in the structure refinement were a scale factor, the a, b, and c lattice parameters, the two variable atomic coordinates y(Cd) and y(Te), two isotropic thermal-motion parameters, four peak-shape parameters, and the preferred orientation parameter. Trial refinements were also carried out in $C2cm$ and $Cmc2_1$, and these gave small additional displacements of ~ 0.003 in x and ~ 0.05 in z, respectively. However, as found in ZnTe-III, these small displacements result in calculated intensities for the very weak (110) and (112) reflections that are clearly larger than those observed. We conclude, therefore, that there is no evidence for symmetry lower than $Cmcm$.

The best $Cmcm$ fit to the profile at 18.6 GPa is shown in Fig. 5. The refined lattice parameters are $a = 5.573(1)$ Å, $b = 5.960(2)$ Å, and $c = 5.284(4)$ Å, and the refined atomic coordinates are y(Cd) $= 0.650(3)$ and y(Te) $= 0.180(3)$. The separation of the atoms along y, Δy, is thus 0.470(4), which is closer to 0.5 than the value of 0.450(1) found in ZnTe-III.[12] To test the significance of the difference from 0.5, refinements were carried out with Δy held at 0.5. This gave clearly poorer fits, with the calculated intensity of (131) reduced nearly to zero and the intensity of (111) halved. In the best-fitting structure, the nearest-neighbor to the Te atom at (0, 0.180, 0.25) is the Cd atom at (0, 0.350, 0.75). As in ZnTe-III, another possible solution to the structure must be considered in which the nearest neighbors are *like* atoms.[12] This distinct structure, which has quite different coordination, was found to give a stable refinement, and a fit that was not clearly unacceptable apart from the (131) reflection which was calculated much weaker than observed. If the atomic coordinates were constrained to give the (131) intensity as observed then larger discrepancies were obtained for other reflections. This alternative is thus excluded in favor of the structure shown in Fig. 6 which is also strongly indicated by the continuous nature of the

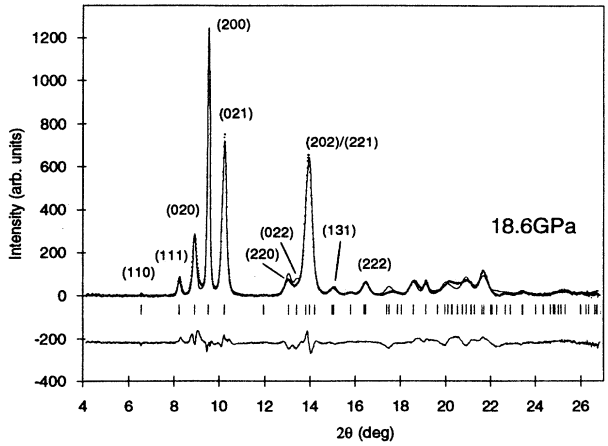

FIG. 5. Fit to the CdTe profile collected at 18.6 GPa. The tick marks show the positions of all the reflections allowed by symmetry, except the omitted (002) reflection (see text). The difference between the observed and calculated profiles is displayed below the tick marks. Apart from (110), very weak reflections have not been indexed.

transition, as discussed below. This best-fitting structure still gives some residual misfits (Fig. 5) which are almost certainly attributable to the inability of a simple, one-parameter model to account completely for the (pronounced) nonaxial preferred orientation.

Figure 6 shows the refined structure at 18.6 GPa projected down (a) the x axis and (b) the z axis. The dashed lines indicate the nearest-neighbor contacts around the Cd atom at (0, 0.650, 0.25) and the Te atom at (0, 0.180, 0.25). The letters label the six different nearest- and next-nearest-neighbor distances which are 2.792(1), 2.801(4), 2.829(2), 3.158(4), 3.190(3), and 3.403(2) Å, in the sequence of a to f. As in ZnTe-III, the structure can

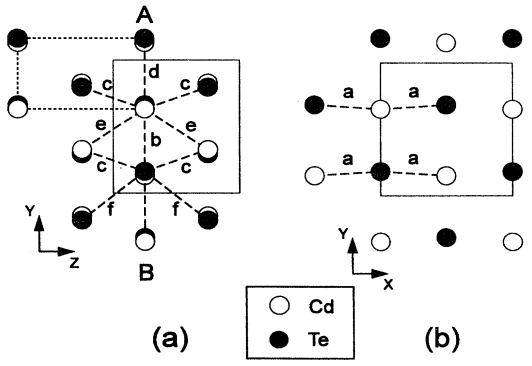

FIG. 6. The $Cmcm$ structure of CdTe at 18.6 GPa. (a) shows a view along the x axis and (b) shows the AB plane in (a) viewed along the z axis. The dashed lines mark the nearest-neighbor contacts around the Cd atom at $(0,0.650,\frac{1}{4})$ and the Te atom at $(0,0.180,\frac{1}{4})$. The letters label the six different nearest- and next-nearest-neighbor distances. The short-dashed rectangle in (a) outlines a $Pmm2$-like pseudocell.

be considered as a distortion of NaCl, with alternate (001) NaCl-like planes of atoms [as in Fig. 6(b)] displaced approximately ± 0.08 along the y axis. Each Cd and Te atom is surrounded by five almost equidistant unlike nearest neighbors at ~ 2.8 Å (two a, one b, and two c contacts), with the nearest of them being those in the buckled chains along the x axis [see a in Fig. 6(b)]. Because $\Delta y \neq 0.5$, the sixth unlike neighbors (the d contacts) are at a significantly greater distance of 3.158 Å. For the Cd atom, this distance is only slightly less than that (e) to the nearest *like* neighbors (3.190 Å), but it is considerably smaller than the shortest Te-Te distance of 3.403 Å (f). The difference between these Cd-Cd and Te-Te distances arises, again, because $\Delta y \neq 0.5$.

Comparison of the *Cmcm* structure with the orthorhombic *Pmm*2 structure proposed previously by Hu[9] reveals that the unit cells are related by $a_c = 2a_p$, $b_c = 2c_p$, $c_c = b_p$, where the subscripts c and p refer to the C-face-centered and primitive orthorhombic cells, respectively. Hu[9] showed that the *Pmm*2 structure gave reasonable agreement with observed reflection intensities, with atoms at (0,0,0) and $(0,\frac{1}{2},\delta=\frac{1}{4})$ referred to the *Pmm*2 cell. This is because the spatial arrangement of atoms in the structure is broadly similar to that of the *Cmcm* structure—except that $\delta \sim 0.17$ rather than $\frac{1}{4}$—as shown in Fig. 6(a), where a *Pmm*2-like pseudocell is outlined by the short-dashed rectangle. However, atoms are all equally spaced along c_p in the *Pmm*2 structure (equiva- lent to $\Delta y = 0.5$ in the *Cmcm* unit cell) and the assumed site ordering of the *Pmm*2 structure makes its (010) planes [i.e., the xy planes of Fig. 6(b)] alternately all Cd and all Te—thus losing the NaCl-like layers that characterize the *Cmcm* structure. These substantial differences lead to the halving of a_c and b_c, which reflections like (111) and (131)—see Fig. 5—plainly show to be incorrect.

Refinements of diffraction profiles collected at pressures below 18.6 GPa confirmed the preliminary assessment (see above) that they too could be fitted using the *Cmcm* structure. Figure 7 shows a *Cmcm* fit to the profile in Fig. 1, which was collected at 11.7 GPa, with $a = 5.761(2)$ Å, $b = 5.834(3)$ Å, $c = 5.715(6)$ Å, $y(\text{Cd}) = 0.722(3)$, and $y(\text{Te}) = 0.235(3)$. The additional features identified in inset (i) of Fig. 1 are all accounted for in this fit, as shown in the inset of Fig. 7. The observed changes above 10 GPa can thus all be understood in terms of a continuous transition of the NaCl structure into the *Cmcm* structure (see note added in proof). The pressure dependence of the a, b, and c lattice parameters of the NaCl and *Cmcm* phases from 4 to 28 GPa is shown in Fig. 8. The unfilled symbols are the data points of Hu,[9] converted to the *Cmcm* unit cell. Figure 9 shows the compression of the unit-cell volume in terms of V/V_0. The continuous onset of the distortion of the cubic NaCl phase is very apparent, with no significant observable discontinuity in either the lattice parameters or the unit-cell volume in the region of the transition.[23] (There also appears to be no change in compressibility at the NaCl to *Cmcm* transition—see Fig. 9.) The continuous lengthening of the b lattice parameter was not detected in the previous work—using film-based techniques on a laboratory x-ray source—because of there being insufficient resolution to observe the (020) reflection below 12.2 GPa, the pressure at which it becomes well separated from (200)—see Fig. 2. If the asymmetry of the (200) reflection at lower pressures is not detected, the continuous transformation from NaCl to *Cmcm* would appear as two separate effects: first the growth of the (021) and (221) reflections, which starts at 10.1 GPa and is indicative of the displacement of alternate (001) planes along the y axis, and then the splitting of the (020) reflection from the (200) reflection becoming discernible at ~ 12.2 GPa as a result of the increased orthorhombic distortion.

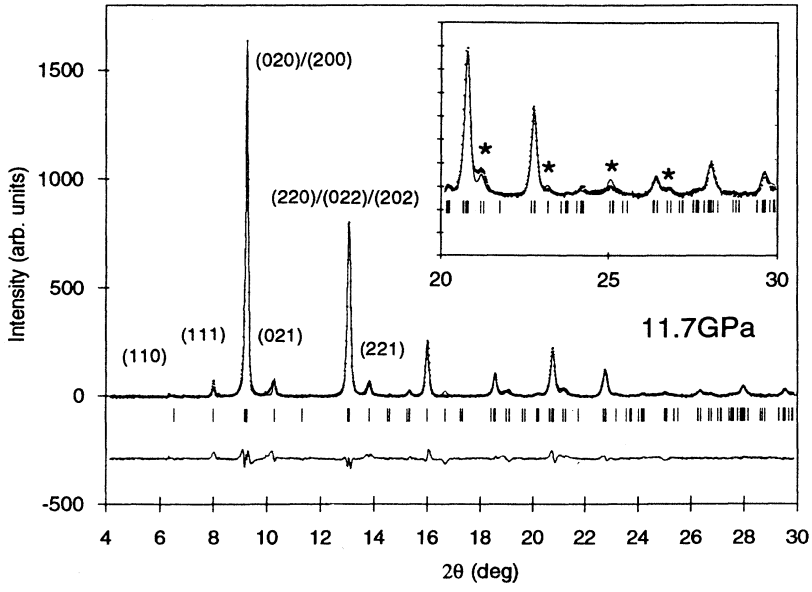

FIG. 7. Fit of the *Cmcm* structure to the CdTe profile collected at 11.7 GPa shown in Fig. 1. The tick marks show the positions of all the reflections allowed by symmetry, except (002) as in Fig. 5. The difference between the observed and calculated profiles is displayed below the tick marks. The inset shows an enlarged view of the high-angle part of the profile, and the asterisks mark the four weak non-NaCl/β-tin reflections identified in the same way in inset (i) of Fig. 1.

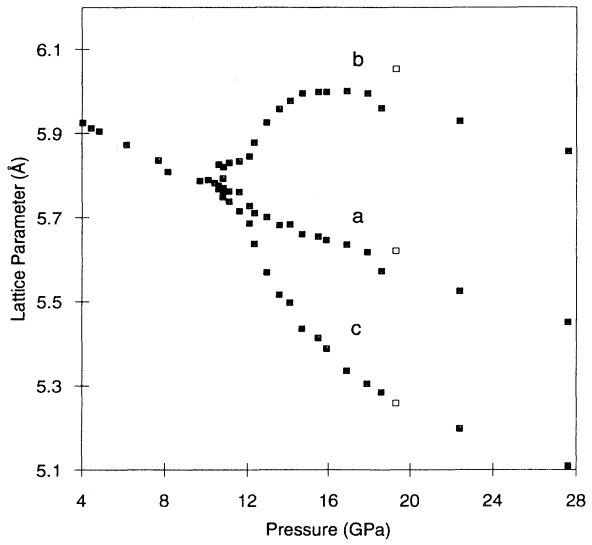

FIG. 8. Pressure dependence of the a, b, and c lattice parameters of the NaCl and *Cmcm* phases of CdTe. The unfilled symbols at 19.3 GPa are the data points from Ref. 9 converted to the *Cmcm* unit cell.

It has been shown previously[9] that above 19.3 GPa the c_p/a_p and b_p/a_p ratios remain fixed at ~ 1.08 and ~ 1.87, respectively. Although it was not explicitly stated in Ref. 9, this implies a b_p/c_p ratio of ~ 1.73 which is very close to $\sqrt{3}$. Such a ratio between the lattice parameters of an orthorhombic structure can indicate a transition to a hexagonal structure, such as we have recently found in Si.[24] As can be seen from Fig. 6(a), the *Cmcm* structure is quasi-simple-hexagonal at 18.6 GPa, but true hexagonal symmetry would require reordering or disordering of the Cd and Te sites. The equivalent to the b_p/c_p ratio in the *Cmcm* structure is $2c_c/b_c$, which is shown as a function of pressure in Fig. 10. Although the value initially decreases rapidly with pressure above the transition, the rate of change becomes less rapid above 16 GPa and the ratio appears to be reaching a limiting value just above $\sqrt{3}$. (And it is shown below that the atomic positions also remain clearly nonhexagonal at 28 GPa—even apart from the site ordering.)

Although it was not possible to carry out Rietveld refinements of the diffraction profiles collected at pressures (10.3 and 10.7 GPa) very close to the NaCl→*Cmcm* transition—because high correlations between structural parameters prevented stable, physically sensible solutions—it was otherwise possible to determine the structural coordinates at all pressures from 10.8 to 28 GPa. The pressure dependence of y(Cd) and y(Te) is shown in Figs. 11(a) and 11(b) and the pressure dependence of Δy, the difference between y(Cd) and y(Te), is given in Fig. 11(c). On compression, the Cd and Te atoms are both displaced along the y axis away from the positions they occupy in the NaCl structure [which can be expressed as a *Cmcm* structure with $a=b=c$, and y(Cd)$=0.75$ and y(Te)$=0.25$]. The structural coordinates mirror the lattice parameters in showing the onset of the orthorhombic distortion to occur mostly over the range up to 16 GPa. Above that there is relatively little change, with y(Cd) and y(Te) remaining at ~ 0.65 and ~ 0.18, respectively—very similar to the coordinates of ZnTe-III at 16 GPa.[12] Figure 11(c) reveals that the relative displacement of the two atoms along y, Δy, also increases in a similar way with pressure, such that the initially straight chains of alternate atoms along the x direction become slightly buckled with increasing pressure, as seen in Fig. 6(b).

As explained above, there is only a small difference in

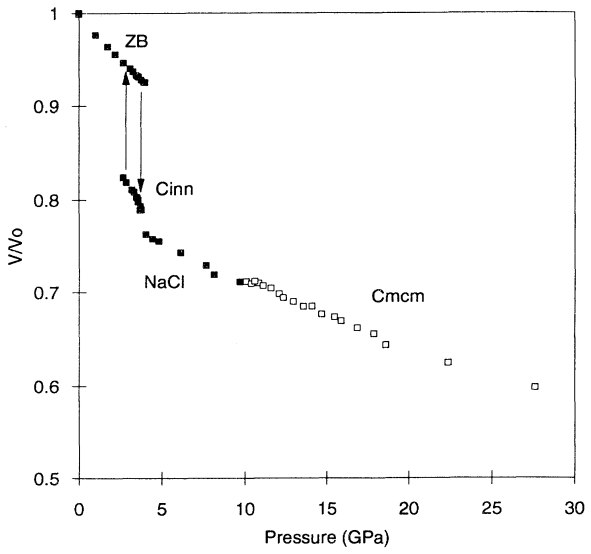

FIG. 9. V/V_0 as a function of pressure for the zincblende (ZB), cinnabar, NaCl, and *Cmcm* phases of CdTe. The data points for the ZB and cinnabar phases are taken from Ref. 11. The two vertical arrows indicate the extent of the hysteresis in the ZB ↔ cinnabar transition, as detailed in Ref. 11. $V_0=68.06$ Å^3 per formula unit.

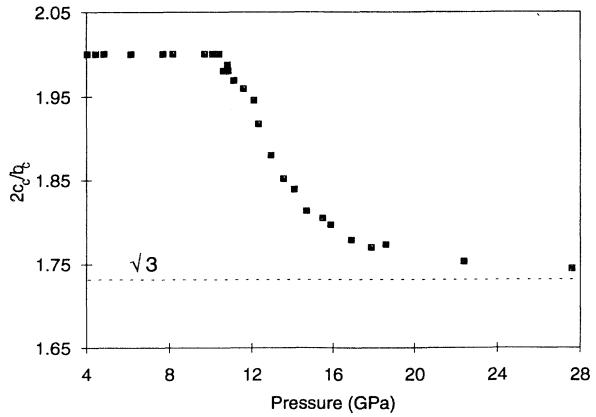

FIG. 10. The pressure dependence of $2c_c/b_c$ ratio in the *Cmcm* and NaCl phases. In the NaCl phase, $2c_c/b_c=2$ by symmetry.

the fit between the structure in Fig. 6 and one in which the nearest-neighbor c contacts link *like* atoms. However, the continuous nature of the distortion from NaCl shows the structure to be as in Fig. 6. The latter has zigzag Cd-Te-Cd-Te chains along z (joined by the c contacts) which arise from the initially straight Cd-Te-Cd-Te chains of the NaCl structure by a continuous relative displacement of Cd and Te in opposite directions along y. In the alternative structure, the c linked chains become zigzag Cd-Cd-Cd-Cd and zigzag Te-Te-Te-Te, which clearly cannot be derived continuously from NaCl without y(Cd) becoming <0.625 and y(Te) becoming <0.125.

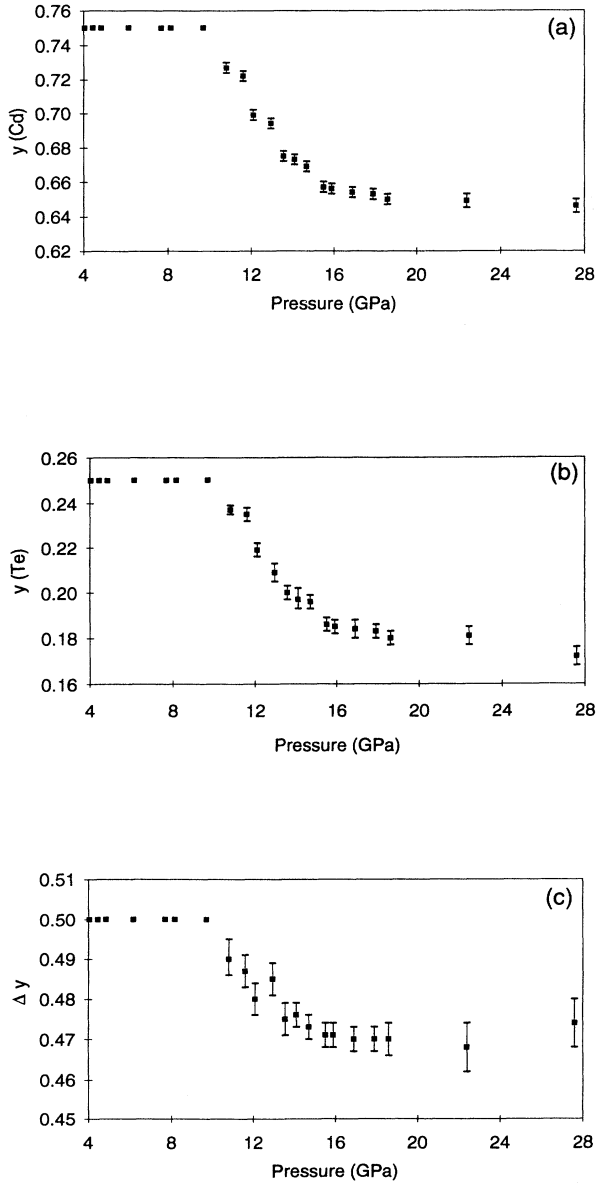

FIG. 11. The pressure dependence of (a) the y(Cd) atomic coordinate, and (b) the y(Te) atomic coordinate in the NaCl and *Cmcm* phases of CdTe. In the NaCl phase, y(Cd)=0.75 and y(Te)=0.25 by symmetry. The relative displacement of the Cd and Te atoms along the y axis, Δy, is shown in (c).

It is worth noting that the *Cmcm* structure is similar to the *Amm*2 structure proposed by Zhang and Cohen for phase II of GaAs,[25] with the y and z axes interchanged. (*Amm*2 then becomes *Cm*2*m*.) Zhang and Cohen remarked that the shearing of alternate NaCl-like planes corresponds to a transverse-acoustic mode of the NaCl structure. The continuous nature of the transition in CdTe could thus be interpreted as a classic soft-mode transition. However, this does not account for the deviations of Δy from 0.5, and this makes the coordination importantly different from that of the *Amm*2 structure.

The effect of the variation of Δy with pressure can be seen in the evolution of the *Cmcm* coordination, as shown in Fig. 12.[26] In the NaCl phase each atom is surrounded by six equidistant unlike atoms at $\sim$2.9 Å, 12 like next-nearest neighbors all at $\sim$4.1 Å, and eight unlike third-nearest neighbors at $\sim$5.1 Å. In the *Cmcm* phase, the pressure dependence of the lattice parameters and the atomic coordinates is such that five of the nearest-neighbor distances remain similar, while the sixth (the d contact) increases sharply as a consequence of the change in Δy from 0.5. If Δy were 0.5, the b and d contacts would *both* become significantly longer than the a and c contacts. $\Delta y \neq 0.5$ is thus necessary to give fivefold rather than fourfold close nearest-neighbor coordination. Above $\sim$20 GPa, the sixth nearest-neighbor distance (d) becomes the same within error as the nearest Cd-Cd distance (e) such that, at 20 GPa, each Cd atom is surrounded by five Te atoms at $\sim$2.77 Å, and a further Te and two Cd atoms at $\sim$3.15 Å. As already pointed out, the change in Δy from 0.5 means that the bonding arrangement around each Te atom is slightly different, with five Cd atoms at $\sim$2.77 Å, the sixth at $\sim$3.15 Å, but with the closest Te atoms significantly further away at 3.37 Å (the f contact).

The perfect sixfold coordination of the NaCl phase has thus been lost in favor of only five close nearest neighbors but with a large reduction in two next-nearest-neighbor distances (e and f) such that the coordination can be viewed as 5+3. The large reduction in the length of the e and f distances arises from the displacement along $\pm y$ of alternate (001) planes, and so is balanced by increases of a similar magnitude in two other next-nearest-neighbor distances, which are labelled j and k in Fig. 12. The relative displacements of neighboring (001) planes also cause the sharp reduction seen in four of the third-nearest-neighbor distances (labelled l), and an equal increase in the other four (m). Thus, at 20 GPa, each atom still has a shell of 12 neighbors at $\sim$4 Å (g,i and l, or h, i, and l), as in the NaCl phase, though these now comprise eight like and four unlike atoms, rather than the 12 like atoms of NaCl. And inside this shell there are now eight neighboring atoms, rather than the six of NaCl. The overall coordination is thus approximately 8+12, which resembles a simple-hexagonal (SH) structure. However, a true SH structure has the b, c, d, e, and f contacts all equal, and the *Cmcm* coordination remains quite different from this

at 20 GPa [and to at least 28 GPa (Ref. 26)], as Fig. 12 makes clear. In any case, as already remarked, the site ordering is inconsistent with hexagonal symmetry.

The bonding arrangement in *Cmcm*-CdTe is thus similar to that observed in ZnTe-III (Ref. 12) which is also 5+3 coordinated, although in that case the *Cmcm* structure occurs after a first-order transition from the cinnabar structure of ZnTe-II. Preliminary results for HgTe show that it also exhibits a first-order transition to the *Cmcm* structure, but from a NaCl phase in that case.[27] Recently, a NaCl phase of ZnTe (ZnTe-IV) has been observed at combined high pressures and high temperatures.[28] It would now be of considerable interest to follow the structural changes that occur with temperature on heating from ZnTe-III to ZnTe-IV—in particular, to determine whether that phase transition is continuous or not.

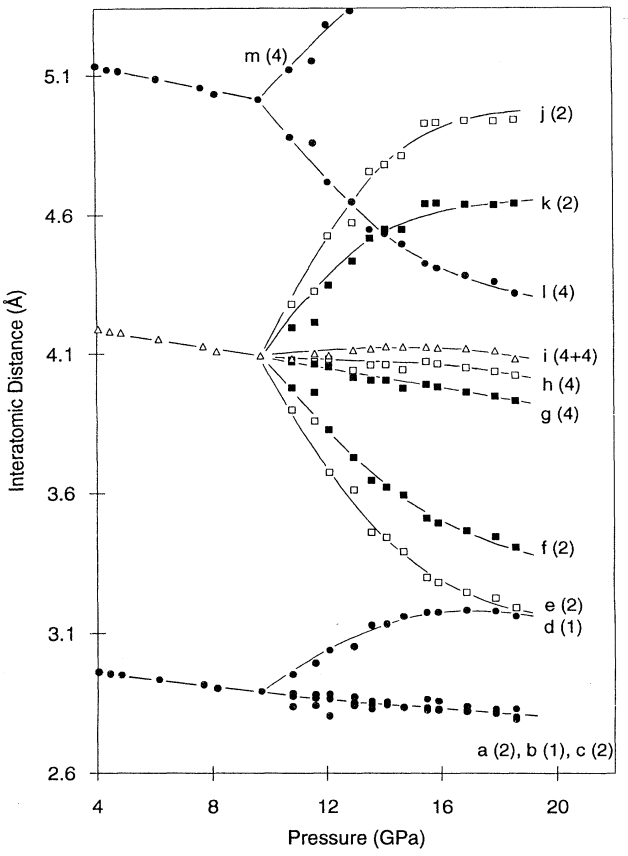

FIG. 12. The pressure dependence of the nearest-, next-nearest-, and third-nearest-neighbor distances in the NaCl and *Cmcm* phases of CdTe. Circles indicate contact distances to unlike atoms, while triangles and squares indicate contact distances to like atoms. The □, ■, and ● symbols indicate Cd-Cd, Te-Te, and Cd-Te contact distances, respectively. The △ symbols used for the *i* contact distance (see below) indicate that this distance is the same for Cd-Cd and Te-Te contacts. All distances are relative to the Cd atom at $(0,0.65,\frac{1}{4})$, denoted Cd_0, and the Te atom at $(0,0.18,\frac{1}{4})$, denoted Te_0. (The specific *y* coordinates given here and in the following are those obtained for the structure at 18.6 GPa, which is as shown in Fig. 6). The distances *a* to *f* are labeled in Fig. 6. The *g* distance is from Te_0 to the Te atom at $(\frac{1}{2},0.32,\frac{3}{4})$; the *h* distance is from Cd_0 to the Cd atom at $(\frac{1}{2},0.85,\frac{3}{4})$; the *i* distance is from Cd_0 and Te_0 to the Cd and Te atoms at $(\frac{1}{2},0.15,\frac{1}{4})$ and $(\frac{1}{2},0.68,\frac{1}{4})$, respectively; the *j* distance is from Cd_0 to the Cd atom at $(0,1.35,\frac{3}{4})$; the *k* distance is from Te_0 to the Te atom at $(0,0.82,\frac{3}{4})$; the *l* distance is from Cd_0 to the Te atom at $(\frac{1}{2},0.32,\frac{3}{4})$; and the *m* distance is from Cd_0 to the Te atom at $(\frac{1}{2},1.32,\frac{3}{4})$. The number in parentheses after the labels *a* to *m* show how many of each type of contact distance there are around each atom. *i* (4+4) indicates four Cd-Cd contact and four Te-Te contacts. The lines through the data points are guides to the eye.

Although the present study has revealed the crystal structure of CdTe above 10 GPa to be more complex than previously believed, the existence of only a single phase, rather than the two phases proposed previously, greatly simplifies the emerging structural systematics of the II-VI materials.[27,29] The observation of both a cinnabar and *Cmcm* structure in ZnTe, CdTe, and a *Cmcm* structure in HgTe, suggests a zincblende→cinnabar →NaCl→*Cmcm* transition sequence in the II-VI tellurides under pressure, although ZnTe appears anomalous in not possessing the NaCl structure at ambient temperature. No evidence has yet been found of a cinnabar phase in the nonmercury II-VI sulfides and selenides, but the reported evidence for a β-tin phase in HgSe (Ref. 1) suggests that it might also have the *Cmcm* structure, and the reported behavior of CdS and CdSe at higher pressures now invites re-examination. Since the more ionic III-V systems are expected to be similar to the II-VI systems in their high-pressure behavior, reported NaCl→β-tin transitions in III-V materials like InAs and InP also attract attention, and preliminary work has given strong evidence that their supposed β-tin phases in fact have the *Cmcm* structure, or something similar to it.[29,30] And the similarity of the *Cmcm* structure to the supposed *Amm*2 structure of GaAs-II (see above) suggests that its true form may also be *Cmcm*-like.[30] It thus appears probable that the continuous nature of the transition in CdTe gives a valuable insight into the nature of a structure type of wide significance in the structural systematics of II-VI and III-V semiconductors.[29]

In summary, our main conclusions are as follows:

(1) CdTe undergoes a continuous phase transition at 10.1 GPa from the NaCl structure to a phase with a site-ordered *Cmcm* structure.

(2) This is the same structure as has been reported recently for phase III of ZnTe, and has the same fivefold coordination of close nearest neighbors.

(3) The *Cmcm* phase is stable from 10 to at least 28 GPa. The previously reported NaCl→β-tin and β-tin→*Pmm*2 transitions, at 10.3 and 12.2 GPa, respectively, are not observed, and can be understood as lower-resolution and lower-sensitivity interpretations of the *Cmcm* powder patter.

Finally, we note that in obtaining these results we have been dependent on the high sensitivity and also the 2-*d* nature of the image-plate data. These make it possible to exploit anomalous dispersion effects, detect very weak reflections and survey preferred orientation, all of which

were needed to reach a satisfactory solution.

Note added in proof. The intrinsically continuous nature of the NaCl→*Cmcm* transition is evident from the gradual splitting of the peak at $2\theta \sim 9°$ in Fig. 2. However, it cannot be ruled out that there may be some phase mixing. At pressures below ~14 GPa, it is difficult in the refinements to distinguish single-phase *Cmcm* from a mixture of NaCl and *Cmcm* phases: both possibilities give similarly good fits to the powder patterns. The mixed-phase refinements yield slightly different atomic coordinates, y(Cd) and y(Te), from those shown in Fig. 11, but the differences are only $\lesssim 0.01$.

ACKNOWLEDGMENTS

We gratefully acknowledge the assistance of our colleague J. S. Loveday in various aspects of the experimental work, and would like to thank A. A. Neild and G. Bushnell-Wye of the Daresbury Laboratory for their help in preparing the beam-line equipment. This work is supported by a grant from the Engineering and Physical Sciences Research Council and by facilities made available by Daresbury Laboratory. Valued assistance with the maintenance and development of pressure cells has been given by D. M. Adams of Diacell Products.

[1]T. Huang and A. L. Ruoff, Phys. Rev. B **31**, 5976 (1985), and references cited therein.

[2]Y. K. Vohra, S. T. Weir, and A. L. Ruoff, Phys. Rev. B **31**, 7344 (1985).

[3]A. San-Miguel, A. Polian, M. Gauthier, and J. P. Itié, Phys. Rev. B **48**, 8683 (1993).

[4]K. Kusaba and D. J. Weidner, in *Proceedings of the Joint AIRAPT/APS Topical Conference on High Pressure Science and Technology, Colorado Springs 1993,* edited by S. C. Schmidt, J. W. Shaner, G. A. Samara, and M. Ross (AIP, New York, 1994), Vol. 1, p. 553.

[5]S. B. Qadri, E. F. Skelton, and A. W. Webb, in *Proceedings of the Joint AIRAPT/APS Topical Conference on High Pressure Science and Technology* (Ref. 4), p. 319.

[6]A. N. Mariano and E. P. Warekois, Science **142**, 672 (1963).

[7]N. B. Owen, P. L. Smith, J. E. Martin, and A. J. Wright, J. Phys. Chem. Solids **24**, 1519 (1963).

[8]I. Y. Borg and D. K. Smith, Jr., J. Phys. Chem. Solids **28**, 49 (1967).

[9]J. Z. Hu, Solid State Commun. **63**, 471 (1987).

[10]R. J. Nelmes, M. I. McMahon, N. G. Wright, and D. R. Allan, Phys. Rev. B **48**, 1314 (1993).

[11]M. I. McMahon, R. J. Nelmes, N. G. Wright, and D. R. Allan, Phys. Rev. B **48**, 16 246 (1993).

[12]R. J. Nelmes, M. I. McMahon, N. G. Wright, and D. R. Allan, Phys. Rev. Lett. **73**, 1805 (1994).

[13]M. I. McMahon, R. J. Nelmes, N. G. Wright, and D. R. Allan, in *Proceedings of the Joint AIRAPT/APS Topical Conference on High Pressure Science and Technology* (Ref. 4), p. 633.

[14]R. J. Nelmes and M. I. McMahon, Adv. X-ray Anal. **37**, 419 (1994).

[15]R. J. Nelmes and M. I. McMahon, J. Synch. Radiat. **1**, 69 (1994), and references cited therein.

[16]D. M. Adams, Diacell Products, 54 Ash Tree Road, Leicester, UK.

[17]H. K. Mao and P. M. Bell, Science **200**, 1145 (1978).

[18]H. M. Rietveld, J. Appl. Crystallogr. **2**, 65 (1969).

[19]A. N. Fitch and A. D. Murray (unpublished).

[20]D. Louër and R. Vargas, J. Appl. Crystallogr. **15**, 542 (1982).

[21]A. March, Z. Kristallogr. **81**, 285 (1932); W. A. Dollase, J. Appl. Crystallog. **19**, 267 (1986).

[22]Other reflections with $l \gg h,k$ are also affected, but only the very strong (002) reflection has a significant effect on the refinement.

[23]Over the pressure range from the transition to ~12.4 GPa, where the (020) and (200) reflections become clearly separated (Fig. 2), there are some significant correlation effects in the lattice-parameter refinements, compounded by the absence from the profiles of the (002) reflection. These featuers very probably account for the apparent underestimate of the a/b and b/c splittings around 12 GPa, and the physically unrealistic small *increase* in $\Delta V/V_0$ just above the transition.

[24]M. I. McMahon, R. J. Nelmes, N. G. Wright, and D. R. Allan, Phys. Rev. B **50**, 739 (1994).

[25]S. B. Zhang and M. L. Cohen, Phys. Rev. B **39**, 1450 (1989).

[26]The results at 22 and 28 GPa have been omitted from Fig. 12 so as to give more space—and hence clarity—to the range immediately above the transition. There are no significant changes in the relative magnitudes of any of the interatomic distances above 20 GPa.

[27]R. J. Nelmes, M. I. McMahon, N. G. Wright, and D. R. Allan, J. Phys. Chem. Solids **56**, 545 (1995).

[28]O. Shimomura (private communication).

[29]M. I. McMahon and R. J. Nelmes, J. Phys. Chem. Solids **56**, 485 (1995).

[30]R. J. Nelmes, M. I. McMahon, N. G. Wright, D. R. Allan, H. Liu, and J. S. Loveday, J. Phys. Chem. Solids **56**, 539 (1995).